Published in final edited form as:
Brain Res. 2006 June 30; 1097(1): 1–10. doi:10.1016/j.brainres.2006.04.046.

Upregulation of DMT1 expression in choroidal epithelia of the blood–CSF barrier following manganese exposure in vitro

Xueqian Wang, **Guojun Jane Li**, and **Wei Zheng**
School of Health Sciences, Purdue University, 550 Stadium Mall Drive, Room 1163D, West Lafayette, IN 47907, USA

Abstract

Divalent metal transporter 1 (DMT1), whose mRNA possesses a stem-loop structure in 3′-untranslated region, has been identified in most organs and responsible for transport of various divalent metal ions. Previous work from this laboratory has shown that manganese (Mn) exposure alters the function of iron regulatory protein (IRP) and increases iron (Fe) concentrations in the cerebrospinal fluid (CSF). This study was designed to test the hypothesis that Mn treatment, by acting on protein–mRNA binding between IRP and DMT1 mRNA, altered the expression of DMT1 in an immortalized choroidal epithelial Z310 cell line which was derived from rat choroid plexus epithelia, leading to a compartmental shift of Fe from the blood to the CSF. Immunocytochemistry confirmed the presence of DMT1 in Z310 cell. Following in vitro exposure to Mn at 100 μM for 24 and 48 h, the expression of DMT1 mRNA in Z310 cells was significantly increased by 45.4% ($P < 0.05$) and 78.1% ($P < 0.01$), respectively, as compared to controls. Accordingly, Western blot analysis revealed a significant increase of DMT1 protein concentrations at 48 h after Mn exposure (100 μM). Electrophoretic mobility shift assay (EMSA) showed that Mn exposure increased binding of IRP to DMT1 mRNA in cultured choroidal Z310 cells. Moreover, real-time RT-PCR revealed no changes in DMT1 heterogeneous nuclear RNA (hnRNA) levels following Mn exposure. These data suggest that Mn appears to stabilize the binding of IRP to DMT1 mRNA, thereby increasing the expression of DMT1. The facilitated transport of Fe by DMT1 at the blood–CSF barrier may partly contribute to Mn-induced neurodegenerative Parkinsonism.

Keywords

Manganese; Choroid plexus; Z310 cell; Blood; CSF barrier; Divalent metal transporter 1; Iron responsive element

1. Introduction

Divalent metal transporter 1 (DMT1), also known as divalent cation transporter 1 (DCT1) or Nramp2 (natural resistance-associated macrophage protein 2), was first identified in mice as a gene homologous to the previously described Nramp (Gruenheid et al., 1995) and subsequently characterized by Gunshin and co-workers as mammalian proton-coupled metal-ion transporter (Gunshin et al., 1997). DMT1, as an integral membrane protein, plays an important role in iron (Fe) transport across the cell membrane (Vidal et al., 1995). In addition, DMT1 nonselectively transports multiple divalent metals including manganese (Mn), copper (Cu), cobalt (Co), zinc (Zn), cadmium (Cd) and lead (Pb) (Gunshin et al.,

Corresponding author. Fax: +1 765 496 1377. wz18@purdue.edu (W. Zheng).

1997). DMT1 is most abundantly expressed in the duodenal epithelia. The expression of DMT1 in other cell types of nearly most of the organs has also been identified including erythrocytes, renal epithelial cells, cardiomyocytes and human placenta epithelia (Ferguson et al., 2001; Georgieff et al., 2000; Ke et al., 2003; Levy et al., 1999). In brain, DMT1 exists in neurons, cerebral capillary endothelial cells that constitute the blood–brain barrier (BBB) and the choroid plexus epithelial cells that comprise the blood–CSF barrier (BCB) (Burdo et al., 2001; Siddappa et al., 2003; Siddappa et al., 2002). The presence of DMT1 in brain barriers is functionally important with regard to the necessity of stable homeostasis of essential elements in brain extracellular fluids for normal brain function. However, the question as to how DMT1 regulates the homeostasis of iron and other metals in the central nervous system (CNS) remains unanswered.

As a trans-membrane protein, the structure of DMT1 possesses two alternate splicing isoforms that result from the mRNA transcripts with distinct alternative 3′-untranslated regions (UTR) (Konarska and Sharp, 1986). There are two major DMT1 mRNA transcripts, one of which contains an iron responsive element (IRE) with a stem-loop structure available for interaction with cellular proteins (Addess et al., 1997; Eisenstein and Ross, 2003; Rouault, 2001). The similar stem-loop structure of IRE has also been identified and characterized in mRNAs encoding transferrin receptor (TfR) (Fig. 1); the latter is important for delivering transferrin-bound iron to CNS via brain capillaries and choroid plexus (Deane et al., 2004). Noticeably, the IRE structure in TfR mRNA binds specifically to a protein known as iron regulatory protein-1 (IRP1), whose active center contains a [4Fe-4S] cluster. In the Fe-deficient condition, IRP1 binds with a high affinity to IRE containing TfR mRNAs, stabilizes TfR expression and increases intracellular levels of TfR (Andrews, 1999; Klausner et al., 1993; Li et al., 2005). It is unclear, however, whether the cellular levels of DMT1 are regulated in the same fashion as the TfR.

Human exposure to manganese results in symptoms highly similar to Parkinson’s disease. Increased use of manganese as a gasoline additive and the ensuing public health hazard have demanded a better understanding of the mechanisms whereby manganese induces neurodegenerative damage. Research from this laboratory has showed that chronic in vivo exposure to manganese, while reducing blood Fe concentrations, increases iron concentrations in the CSF, suggesting a likely compartment shift of iron from the blood circulation to brain extracellular fluids (Zheng et al., 1999). Our recent in vitro studies have further demonstrated an increased iron transport at the blood–CSF barrier (Li et al., 2005), a result that may be due to manganese interference on iron regulatory mechanism at the choroid plexus. From the chemistry point of view, manganese ions have many biochemical properties in common with iron including ionic radius, electrical charges in biological matrices, binding affinity for the carrier protein and subcellular accumulation in mitochondria (Aschner et al., 1999; Chen et al., 2001; Zheng et al., 1998). Because of these similarities, manganese may compete with iron in IRP1 and thus alter the binding activity of IRP1 to the stem-loop containing TfR mRNAs (Chen et al., 2001; Zheng et al., 1998). Since the mRNA encoding DMT1 contains a stem-loop structure, we hypothesized that manganese exposure may alter the binding of IRPs to DMT1 mRNA, thereby altering DMT1 expression in the choroid plexus; this could contribute to a distorted iron homeostasis in the CSF.

The aims of this study were (1) to verify the existence of DMT1 in Z310 cells, a new cell line derived from rat choroidal epithelial cells (Zheng and Zhao, 2002), (2) to investigate whether manganese exposure altered the DMT1 expression by using real-time RT-PCR to examine the expression of DMT1 mRNA and by Western blot analysis to determine DMT1 protein levels and (3) to study the effect of manganese exposure on protein–mRNA interactions between IRPs and DMT1 mRNA by electrophoretic mobility shift assay (EMSA).

2. Results

2.1. The presence of DMT1 in Z310 cell line by immunocytochemistry

Immunocytochemical studies demonstrated the presence of DMT1 in Z310 cells (Fig. 2B). The punctate DMT1 staining was visibly present in cytoplasm. The control in the absence of primary antibody against DMT1 showed a negative staining (Fig. 2A).

2.2. Manganese exposure increases mRNA and protein levels of DMT1 in vitro

Real-time RT-PCR assay confirmed the presence of mRNA encoding DMT1 in the cultured Z310 cells. Quantitation by the real-time RT-PCR revealed that manganese treatment at 100 μM for 24 h and 48 h significantly increased the levels of DMT1 mRNA by 45.4% and 78.1%, respectively, as compared to the control ($P < 0.05$, Fig. 3). Treatment with 50 μM desferrioxamine (DFOM), an iron chelator, for 10 h, also resulted in a significant increase in DMT1 mRNA (Fig. 3). The increase of DMT1 mRNA level in Z310 cells appeared to be concentration-related within the range of 100–200 μM ($r = 0.870$. $P < 0.01$, Fig. 4). To verify if the increased DMT1 mRNA level was indeed associated with an altered DMT1 protein in Z310 cells, the Western blot analysis was used to separate and quantify DMT1 proteins. Following manganese exposure at 100 μM for 48 h, a significant increase in cellular protein levels of DMT1 was observed ($P < 0.05$, Fig. 5). Noticeably, the antibody used in this experiment was against the C-terminal from 552 to 570 amino acid of DMT1, which is a distinguished part of DMT1 isoform I (Lee et al., 1998; Roth et al., 2000). Thus, the single band with an estimated molecular weight of 65 kDa represents DMT1 proteins.

2.3. Manganese exposure increases IRP binding to DMT1 mRNA in vitro

The increased protein level of DMT1 by manganese treatment could be due to manganese action at the transcriptional level to increase DMT1 gene expression or due to manganese modulation at the translational level to stabilize DMT1 protein expression. Since DMT1 mRNA has the stem-loop structure for IRP binding, it is possible that manganese treatment may enhance the binding of cytosolic IRPs to radiolabeled DMT1-IRE sequences. The EMSA results showed that manganese treatment did increase the binding of IRP1 to DMT1-IRE sequence as evidenced by (i) an increased density of protein–mRNA band on gels (Figs. 6A, B), (ii) a reduced density of this band in the presence of excess unlabeled DMT1-IRE sequences (Fig. 6C) and (iii) a shifted band when the cytosolic preparation was pretreated with antibody against IRP1 (Fig. 6D). Thus, it appears likely that manganese stabilizes the binding of IRP1 to DMT1 mRNA, thereby increasing the expression of DMT1 proteins.

2.4. Manganese exposure did not alter the status of DMT1 heterogeneous nuclear RNA (hnRNA)

The hnRNA represents newly transcribed, unspliced RNA and presents in a small percentage of total RNA in the nucleus of the cell (Danzi et al., 2003). Only after properly spliced and processed does hnRNA become mRNA and enter the cytoplasm (Konarska and Sharp, 1986). Therefore, the levels of hnRNA reflect the rate of gene transcription and RNA processing. To investigate whether manganese exposure affected DMT1 gene transcription, the levels of DMT1 hnRNA were determined by real-time RT-PCR. The amount of DMT1 hnRNA was normalized by the expression of β-actin hnRNA. Results showed that manganese treatment (50, 100 or 200 μM for 24 h) did not lead to any statistically significant changes in the expression of DMT1 hnRNA, as compared to the control group (Fig. 7). Thus, it seemed unlikely that manganese altered DMT1 expression by acting on transcription of DMT1 DNA.

3. Discussion

The presence of DMT1 in the choroid plexus, the tissue where the blood–CSF barrier is located, has been demonstrated in the tissues from rats, mice and humans (Choudhuri et al., 2003; Gunshin et al., 1997; Kishi and Tabuchi, 1997; Knutson et al., 2004; Miller, 2004; Moos and Morgan, 2004; Siddappa et al., 2002). Z310 cells were immortalized cells directly derived from rat choroidal epithelia (Zheng and Zhao, 2002). Our current study by using immunocytochemical staining, Western blot and real-time RT-PCR techniques confirms the presence of DMT1 in this established choroidal epithelial cell line.

Regulation of iron homeostasis in the body has long been regarded as a transferrin (Tf)-mediated process. However, studies in the last decade suggest that non-transferrin-mediated mechanisms may also play a significant role in regulation of iron homeostasis. For example, animal models with DMT1 mutation, such as *mk* mice and Belgrade rats, have shown the defects in iron transport function, leading to anemia (Fleming et al., 1998; Fleming et al., 1997; Gruenheid et al., 1999; Su et al., 1998). Studies on brain barriers have also suggested that iron can be transported across the BBB and BCB into the CNS through a non-Tf-mediated transport (Bradbury, 1997; Moos and Morgan, 2004; Takeda et al., 2002). A recent study from this laboratory by using brain perfusion technique demonstrates that non-transferrin-bound iron can get access to the CSF en route the choroid plexus by a yet unidentified mechanism (Deane et al., 2004). Our observation of the presence of DMT1 in the choroidal Z310 cells is consistent with these earlier reports. Thus, it is highly likely that DMT1 may act as the transporter for free iron at the BCB.

Manganese-induced neurotoxicities could be due to the distorted iron metabolism at both systemic and cellular levels (Chen et al., 2001; Zheng et al., 1998, 1999; Zheng and Zhao, 2001). An increased TfR expression and ensuing elevated iron transport at the BCB may partly explain the disrupted iron status in the CSF (Li et al., 2005). In the current study, we observed that, in addition to action on TfR, manganese exposure increased DMT1 levels in cultured choroidal epithelial cells. Real-time RT-PCR results revealed that the increase in DMT1 mRNA level was manganese dose-dependent and exposure time-associated. Western blot analyses further substantiated manganese-induced elevated protein level of DMT1 in the choroid plexus. While manganese exposure evidently causes the upregulation of TfR and DMT1 in the BCB, the questions as to which direction iron or manganese ions are transported by these two transporters and by what extent each transporter may contribute to a raised iron level in the CSF remain unanswered. Thus, much more work needs to be done to explore these mechanisms.

Increased DMT1 protein level following manganese exposure could be due to manganese action at the transcriptional level to increase DMT1 RNA production and/or RNA processing or at the post-transcriptional level by blocking DMT1 mRNA degradation. The mRNA encoding DMT1 contains a unique IRE stem-loop structure, which is subjected to the binding of cellular IRP1. Under iron sufficient condition, IRP1 possesses the [4Fe-4S] cluster in its active center and functions as aconitase to convert isocitrate in the tricarboxylic acid cycle. When the cells are in need of iron, the [4Fe-4S] configuration is turned into [3Fe-4S], which favors the protein to bind to IRE-containing mRNA including TfR mRNA (Rouault and Klausner, 1996; Zheng et al., 1998). Earlier work from this laboratory has demonstrated that manganese, by replacing one iron in the [4Fe-4S] in IRP1, inhibits the enzyme's catalytic function and increases its binding activity to IRE-containing TfR mRNA; the event leads to an increased expression of TfR (Li et al., 2005; Zheng et al., 1998). In this study, we used EMSA to determine the binding activity between cellular IRP1 and DMT1 mRNA whose sequence contains a stem-loop similar to TfR mRNA at 3′-UTR. When choroidal epithelial cells were exposed to manganese, a significant increase in binding of

IRP1 to DMT1 stem-loop mRNAs was observed. Since the binding of IRP1 to IRE in DMT1 mRNA protects the mRNA sequence from degradation, it is reasonable to postulate that Fe–Mn interaction at the IRP1 may facilitate the binding of IRP1 to DMT1 mRNA, subsequently increase DMT1 mRNA stability and lead to the overproduction of DMT1 protein. The exact structural interaction between IRP proteins and IRE-containing DMT1 mRNAs awaits further exploration. However, our results are consistent with the studies conducted by Gunshin et al. (2001), who have shown that DMT1 mRNA is regulated through stabilization by the IRE-IRP system, in an analogy to TfR regulation. Although the direction of iron transport that is regulated by DMT1 at the BCB remains unknown, the alteration of iron homeostasis in the CSF appeared to be the net result of IRP1-regulated events involving both TfR and DMT1. Noticeably, IRP2 also binds to the IRE motif to modulate iron homeostasis (Guo et al., 1995; Siddappa et al., 2003). As reported recently, while both IRP1 and IRP2 are required for tissue iron regulation in vivo, in most cell lines, IRP1 seems to be a predominant factor in this protein–mRNA interaction in response to cellular iron status (Meyron-Holtz et al., 2004).

The elevated level of DMT1 mRNA by manganese treatment could also result from manganese action at DNA transcriptional level or due to upregulation of DMT1 mRNA. The hnRNA is the primary transcripts directly transcripted from genomic DNA. The hnRNA analysis is a useful technique to determine whether manganese acts on the gene transcription of DMT1. By assessing DMT1 hnRNA, we found no significant changes in DMT1 hnRNA levels following manganese exposure. Thus, it appears unlikely that the action of manganese on cellular DMT1 status is due to manganese action on DMT1 gene modulation.

In summary, the results of this study indicate that manganese exposure increases DMT1 expression in the blood–CSF barrier. Manganese treatment appears to increase the binding ability of cellular IRP1 to IRE-containing DMT1 mRNA, stabilize the DMT1 mRNA and promote the expression of DMT1 protein. The combined effect of DMT1 and TfR on iron transport at the BBB and BCB may contribute to manganese-elicited compartmental shift of iron from the blood to the CSF in manganese-induced neurodegenerative diseases.

4. Experimental procedures

4.1. Cell culture and treatment

The Z310 choroidal epithelial cell line was established from murine choroid plexus and used in the experiments. The detailed procedure for cell culture and maintenance can be found in the previous publications (Li et al., 2005; Zheng and Zhao, 2002). In short, the cells were grown in Dulbecco's modified Eagle's medium (DMEM) supplemented with 10% fetal bovine serum (FBS) in a humidified incubator with 95% air–5% CO_2 at 37 °C. Mn (II) solution as $MnCl_2$ was prepared by directly dissolving $MnCl_2$ salts in distilled, deionized water at a concentration of 40 mM as the stoking solution. The working solutions were diluted from the stock on the day of use. The cells were exposed to 50, 100 or 200 μM Mn for 24 h for dose–response study or 100 μM Mn for 12, 24 or 48 h for time course study. The dose regimen chosen as such was based on previous research in this particular area by this group or others (Li et al., 2005; Reaney and Smith, 2005; Zheng et al., 1999). To create iron overloaded and iron deficiency conditions, cells were exposed to 20 μM hemin and 50 μM DFOM for 10 h, respectively.

4.2. Immunocytochemistry

The cells to be stained were cultured on a chamber for 2–3 days (Lab-Tek II chamber slide system, VWR). The cells were fixed in 4% paraformaldehyde in PBS solution followed by 3 washes with phosphate-buffered saline (PBS). The cell monolayer attached to a glass coverslip was pretreated with 0.3% hydrogen peroxide in methanol for 30 min at room

temperature and incubated with 10% goat serum for 30 min. The cells were incubated with rabbit anti-rat DMT1 antibody (5 μg/ml) in PBS at room temperature for 30 min and rinsed with PBS for 3 times. The cultures were then incubated with biotinylated goat anti-rabbit secondary antibody (1:200) in PBS for 30 min. The negative control was stained with only secondary antibody. The specimens were further washed with PBS, stained with ABC reagent (VECTASTAIN, Vector Laboratories, UK) to form avidin–biotin–horseradish peroxidase complex. HRP was visualized using the substrate 3,3-diaminobenzidine (DAB, Vector Laboratories, UK) and examined under a microscope.

4.3. Western blot analysis of DMT1

Western blot experiments were carried out as previously described (Ke et al., 2003). In short, cellular proteins were extracted in homogenization buffer containing 20 mM Tris, pH 7.5, 5 mM EGTA, 1% Triton X-100, 0.1% SDS, Protease Inhibitor Cocktail (Calbiochem, San Diego, CA). Samples were sonicated and assayed for protein concentrations by Bradford protein assay. A volume of protein extracts (40 μg of protein) was mixed with an equal volume of 2× sample buffer (0.125 M Tris, 4% SDS, 20% glycerol, 0.2% 2-mercaptoethanol, 0.01% bromo-phenol blue) and run on a 4–20% Tris–HCl linear gradient ready gel, electrophoresed and transferred to a PVDF membrane. The membrane was blocked with 5% dry milk in TBS (Tris-buffered saline) and incubated with an antibody directly against DMT1 with IRE (ADI, San Antonio, CA). The membrane was stained with a horseradish-peroxidase-conjugated goat anti-rabbit IgG antibody (1:2000) and developed using enhanced chemiluminescence (ECL, Amersham Biosciences, NJ). β-actin (42 kDa) was used as an internal control. Band intensity was quantified using UN-SCAN-IT™ (Version 5.1) software (Silk Scientific Inc., Orem, Utah).

4.4. Electrophoretic mobility shift assay (EMSA)

EMSA was conducted to determine the interaction between IRPs and mRNAs containing IRE according to manufacturer's direction (Fermentas Life Science, Hanover, MD). The procedure consisted of four major steps.

(1) Extraction of S100 cytoplasmic protein—Z310 cells with or without manganese exposure were harvested and homogenized followed by centrifugation at 100,000 × *g* for 1 h. The supernatant was dialyzed for 8 h against 20 volumes of degassed dialysis buffer composed of 20 mM HEPES, 0.1 M KCl, 20% (v/v) glycerol, 0.2 mM EDTA, 0.5 mM PMSF, and 0.5 mM dithiothreitol (DTT) using Spectra/Pro 16-well MicroDialyzer (150 μl capacity, Spectrum Laboratories, Rancho Dominguez, CA). The S100 cytoplasmic extracts were stored at −80 °C until use (Lin et al., 2001).

(2) Preparation of RNAs containing stem-loop structure—The DNA oligonucleotide template T7-1 (sequence: 5′-TAATA CGACTC ACTATA-3′) was annealed to DMT1-IRE (2 μM) (sequence: 5′-AAC CAT AGA AAC ACA CTG GCT CTG ATG GCT TCT CCC TAT AGT GAG TCG TAT TA-3′) (customer synthesized by IDT, Coralville, IA) in 50 μl anneal buffer (10 mM Tris–HCl pH 7.5, 10 mM $MgCl_2$) (Gunshin et al., 2001). The mixture was heated to and maintained at 95 °C for 5 min and then cooled to less than 35 °C before operating the next step. The transcription reaction was carried out in a total of 20 μl with 2 μl annealed template, 1 μl T7 RNA polymerase (20 units), 1 μl of ribonuclease inhibitor, 1 μl of 10 mM ATP, GTP and CTP mix, 2.4 μl 100 μM UTP and 5 μl of [α-^{32}P] UTP (50 μCi at 10 mCi/ml) for 1 h at 37 °C followed by RNA precipitation in chloroform. The labeled RNAs containing DMT1 stem-loop structure were frozen at −80 °C until use.

(3) EMSA—The S100 cytoplasmic extracts were incubated with [^{32}P]-labeled DMT1-IRE-containing RNA in a band shift buffer (25 mM K-HEPES pH 7.6 at 25 °C, 150 mM CH_3COOK, 1.5 mM Mg Cl_2, 5% glycerol) at 22 °C for 30 min. RNA–protein complexes were separated by electrophoresis on a nondenaturing 6% polyacrylamide gel at 100 V for 3 h. After drying, the gels were exposed to Kodak BioMax XAR film. The density of protein–RNA bound bands was quantified using UN-SCAN-ITTM gel Version 5.1 software.

(4) Competition assay and supershift assay—The competition reaction was prepared as follows, [^{32}-P] labeled DMT1-IRE was mixed with either 1×, 2× or 3× excess of unlabeled competitor RNA. The mixture was incubated with S100 cytoplasmic extracts at 22 °C for 30 min and run on gel. Supershift was performed by adding IRP1 antibody (a kind gift from Dr. Tracey A. Rouault, NICHD) and IRP2 antibody (a kind gift from Dr. Elizabeth A. Leibold, University of Utah.) into the reaction system. The bands were obtained in the same method as described before.

4.5. Determination of heterogeneous nuclear RNA (hnRNA)

The first product of transcription is the primary transcript or hnRNA, which includes both introns and exons. Total RNA from Z310 cells was used in reverse transcription reaction with a reverse primer (5′-ATTGCCACCGCTGGTATCTT-3′; GenBank accession no. AF008439) that corresponds to intronic sequence. DNase I was used to digest DNA. RT-PCR was performed with both forward primer (5′-ATTGCCATCATCCC-TACCCT-3′; GenBank accession no. AF008439) that corresponds to exonic sequence and reverse primer as above. These primers amplified only DMT1 hnRNA. After an initial activation step at 95 °C for 15 min, amplification was done with 40 cycles; melting step at 95 °C for 30 s; annealing at 60 °C for 1 min; and extension at 72 °C for 30 s. An aliquot (20 μl) of the PCR reaction product was run on a 2% agarose gel with ethidium bromide. β-actin hnRNA was used as an internal control (Danzi et al., 2003). All RT-PCR reactions were done in triplicates.

4.6. Quantitative real-time RT-PCR analysis DMT1 mRNA

Levels of DMT1 mRNA were quantified using real-time RT-PCR analysis as described by Walker (2001). Briefly, total RNA was isolated from Z310 cells using Tri-Reagent following the manufacturer's direction (Molecular Research Center, Cincinnati, OH). An aliquot (2 μg) of RNA was reverse-transcribed with MuLV reverse transcriptase (Applied Biosystems, Foster City, CA) and oligo-dT primers. The forward and reverse primers for selected genes were designed using Primer Express 2.0 software (Applied Biosystems, Foster City, CA). The ABsolute QPCR SYBR green Mix kit (ABgene, Rochester, New York) was used for real-time RT-PCR analysis. The amplification was carried out in the Mx3000P Real-Time PCR System (Stratagene, La Jolla, CA). Amplification conditions were 15 min at 95 °C followed by 40 cycles of 30 s at 95 °C, 1 min at 60 °C and 30 s at 72 °C.

Primers sequences used for real-time RT-PCR analysis were: for rat DMT1 using a forward primer 5′-CAG TGC TCT GTA CGT AAC CTG TAA GC-3′ and reverse primer 5′-CGC AGA AGA ACG AGG ACC AA-3′ (GenBank accession no. AF008439), which specifically amplified DMT1 containing IRE; for rat GAPDH, used as an internal control, using a forward primer 5′-CCT GGA GAA ACC TGC CAA GTA T-3′ and reverse primer 5′-AGC CCA GGA TGC CCT TTA GT-3′ (GenBank accession no. NM_017008).

The relative differences in gene expression between groups were expressed using cycle time (Ct) values; these Ct values of the interested genes were first normalized with that of GAPDH in the same sample, and then the relative differences between control and treatment

groups were calculated and expressed as relative increases setting the control as 100%. Assuming that the Ct value is reflective of the initial starting copy and that there is 100% efficiency, a difference of one cycle is equivalent to a two-fold difference in starting copy (Liu et al., 2004a,b; Livak and Schmittgen, 2001; Walker, 2001).

4.7. Statistical analysis

All data are expressed as mean ± SE. The replicates of experiments conducted in the same day were referred as $n = 1$; three or four such replicates on different dates were used for statistical analyses. Statistical analyses of the differences between groups were carried out by one-way ANOVA using SPSS 12.0 statistic package for Windows. The differences between two means were considered significant if P values were equal or less than 0.05.

4.8. Materials

Chemicals were obtained from the following sources: DMEM, fetal bovine serum (FBS), penicillin and streptomycin, gentamycin, RNase-free DNase I and 0.25% Trypsin-1 mM EDTA (TE) from Invitrogen Life Technologies (Carlsbad, CA); rabbit anti-rat DMT1 antibody from Alpha Diagnostic International (San Antonio, CA); ATP, GTP, CTP and UTP (NTPs), [α-^{32}P]UTP, T7 polymerase and peroxidase-labeled anti-rat secondary antibody from Amersham (Piscataway, NJ); SDS from Bio-Rad (Hercules, CA); bromophenol blue from Fisher Scientific Company (Fair Lawn, NJ); dithiothreitol (DTT), DFOM, hemin, EDTA, HEPES, 2-mercaptoethanol, paraformaldehyde, phenyl-methylsulfonyl fluoride (PMSF), polyacrylamide, tetramethyl-ethylenediamine (TEMED), Triton X-100 and all other chemicals from Sigma Chemicals (St. Louis, MO). All reagents were of analytical grade, HPLC grade or the best available pharmaceutical grade.

Acknowledgments

We are grateful to Dr. Chaoying Zhang (University of Toronto, Canada) for kindly designing DMT1 hnRNA primers, Dr. Jie Liu (National Cancer Institute) for designing DMT1 mRNA primers, Dr. Tracey A. Rouault (National Institute of Child Health and Human Development) for providing IRP1 antibody and Dr. Elizabeth A. Leibold (University of Utah) for providing IRP2 antibody at our request. This study was supported by NIH/ National Institute of Environmental Health Sciences grant ES08164 and ES013118 and Johnson and Johnson Focus Program.

Abbreviations

BBB	blood–brain barrier
BCB	blood–cerebrospinal fluid barrier
CSF	cerebrospinal fluid
DFOM	desferrioxamine
DMT1	divalent metal transporter 1
EMSA	electrophoretic mobility shift assay
Fe	iron
hnRNA	heterogeneous nuclear RNA
IRE	iron responsive element
IRP	iron regulatory protein

References

Addess KJ, Basilion JP, Klausner RD, Rouault TA, Pardi A. Structure and dynamics of the iron responsive element RNA: implications for binding of the RNA by iron regulatory binding proteins. J Mol Biol. 1997; 274:72–83. [PubMed: 9398517]

Andrews NC. The iron transporter DMT1. Int J Biochem Cell Biol. 1999; 31:991–994. [PubMed: 10582331]

Aschner M, Vrana KE, Zheng W. Manganese uptake and distribution in the central nervous system (CNS). Neurotoxicology. 1999; 20:173–180. [PubMed: 10385881]

Bradbury MW. Transport of iron in the blood–brain–cerebrospinal fluid system. J Neurochem. 1997; 69:443–454. [PubMed: 9231702]

Burdo JR, Menzies SL, Simpson IA, Garrick LM, Garrick MD, Dolan KG, Haile DJ, Beard JL, Connor JR. Distribution of divalent metal transporter 1 and metal transport protein 1 in the normal and Belgrade rat. J Neurosci Res. 2001; 66:1198–1207. [PubMed: 11746453]

Chen JY, Tsao GC, Zhao Q, Zheng W. Differential cytotoxicity of Mn(II) and Mn(III): special reference to mitochondrial [Fe-S] containing enzymes. Toxicol Appl Pharmacol. 2001; 175:160–168. [PubMed: 11543648]

Choudhuri S, Cherrington NJ, Li N, Klaassen CD. Constitutive expression of various xenobiotic and endobiotic transporter mRNAs in the choroid plexus of rats. Drug Metab Dispos. 2003; 31:1337–1345. [PubMed: 14570765]

Danzi S, Ojamaa K, Klein I. Triiodothyronine-mediated myosin heavy chain gene transcription in the heart. Am J Physiol Heart Circ Physiol. 2003; 284:H2255–H2262. [PubMed: 12609823]

Deane R, Zheng W, Zlokovic BV. Brain capillary endothelium and choroid plexus epithelium regulate transport of transferrin-bound and free iron into the rat brain. J Neurochem. 2004; 88:813–820. [PubMed: 14756801]

Eisenstein RS, Ross KL. Novel roles for iron regulatory proteins in the adaptive response to iron deficiency. J Nutr. 2003; 133:1510S–1516S. [PubMed: 12730455]

Ferguson CJ, Wareing M, Ward DT, Green R, Smith CP, Riccardi D. Cellular localization of divalent metal transporter DMT-1 in rat kidney. Am J Physiol Renal Physiol. 2001; 280:F803–F814. [PubMed: 11292622]

Fleming MD, Trenor CC III, Su MA, Foernzler D, Beier DR, Dietrich WF, Andrews NC. Microcytic anaemia mice have a mutation in Nramp2, a candidate iron transporter gene. Nat Genet. 1997; 16:383–386. [PubMed: 9241278]

Fleming MD, Romano MA, Su MA, Garrick LM, Garrick MD, Andrews NC. Nramp2 is mutated in the anemic Belgrade (b) rat: evidence of a role for Nramp2 in endosomal iron transport. Proc Natl Acad Sci U S A. 1998; 95:1148–1153. [PubMed: 9448300]

Georgieff MK, Wobken JK, Welle J, Burdo JR, Connor JR. Identification and localization of divalent metal transporter-1 (DMT-1) in term human placenta. Placenta. 2000; 21:799–804. [PubMed: 11095929]

Gruenheid S, Cellier M, Vidal S, Gros P. Identification and characterization of a second mouse Nramp gene. Genomics. 1995; 25:514–525. [PubMed: 7789986]

Gruenheid S, Canonne-Hergaux F, Gauthier S, Hackam DJ, Grinstein S, Gros P. The iron transport protein NRAMP2 is an integral membrane glycoprotein that colocalizes with transferrin in recycling endosomes. J Exp Med. 1999; 189:831–841. [PubMed: 10049947]

Gunshin H, Mackenzie B, Berger UV, Gunshin Y, Romero MF, Boron WF, Nussberger S, Gollan JL, Hediger MA. Cloning and characterization of a mammalian proton-coupled metal-ion transporter. Nature. 1997; 388:482–488. [PubMed: 9242408]

Gunshin H, Allerson CR, Polycarpou-Schwarz M, Rofts A, Rogers JT, Kishi F, Hentze MW, Rouault TA, Andrews NC, Hediger MA. Iron-dependent regulation of the divalent metal ion transporter. FEBS Lett. 2001; 509:309–316. [PubMed: 11741608]

Guo B, Phillips JD, Yu Y, Leibold EA. Iron regulates the intracellular degradation of iron regulatory protein 2 by the proteasome. J Biol Chem. 1995; 270:21645–21651. [PubMed: 7665579]

Ke Y, Chen YY, Chang YZ, Duan XL, Ho KP, Jiangde H, Wang K, Qian ZM. Post-transcriptional expression of DMT1 in the heart of rat. J Cell Physiol. 2003; 196:124–130. [PubMed: 12767048]

Kishi F, Tabuchi M. Complete nucleotide sequence of human NRAMP2 cDNA. Mol Immunol. 1997; 34:839–842. [PubMed: 9464519]

Klausner RD, Rouault TA, Harford JB. Regulating the fate of mRNA: the control of cellular iron metabolism. Cell. 1993; 72:19–28. [PubMed: 8380757]

Knutson M, Menzies S, Connor J, Wessling-Resnick M. Developmental, regional, and cellular expression of SFT/UbcH5A and DMT1 mRNA in brain. J Neurosci Res. 2004; 76:633–641. [PubMed: 15139022]

Konarska MM, Sharp PA. Electrophoretic separation of complexes involved in the splicing of precursors to mRNAs. Cell. 1986; 46:845–855. [PubMed: 2944598]

Lee PL, Gelbart T, West C, Halloran C, Beutler E. The human Nramp2 gene: characterization of the gene structure, alternative splicing, promoter region and polymorphisms. Blood Cells Mol Dis. 1998; 24:199–215. [PubMed: 9642100]

Levy JE, Jin O, Fujiwara Y, Kuo F, Andrews NC. Transferrin receptor is necessary for development of erythrocytes and the nervous system. Nat Genet. 1999; 21:396–399. [PubMed: 10192390]

Li GJ, Zhao Q, Zheng W. Alteration at translational but not transcriptional level of transferrin receptor expression following manganese exposure at the blood–CSF barrier in vitro. Toxicol Appl Pharmacol. 2005; 205:188–200. [PubMed: 15893546]

Lin E, Graziano JH, Freyer GA. Regulation of the 75-kDa subunit of mitochondrial complex I by iron. J Biol Chem. 2001; 276:27685–27692. [PubMed: 11313346]

Liu J, Walker N, Waalkes MP. Hybridization buffer systems impact the quality of filter array data. J Pharmacol Toxicol Methods. 2004a; 50:67–71. [PubMed: 15233970]

Liu J, Xie Y, Ward JM, Diwan BA, Waalkes MP. Toxicogenomic analysis of aberrant gene expression in liver tumors and nontumorous livers of adult mice exposed in utero to inorganic arsenic. Toxicol Sci. 2004b; 77:249–257. [PubMed: 14691202]

Livak KJ, Schmittgen TD. Analysis of relative gene expression data using real-time quantitative PCR and the 2 (-Delta Delta C(T)) method. Methods. 2001; 25:402–408. [PubMed: 11846609]

Meyron-Holtz EG, Ghosh MC, Rouault TA. Mammalian tissue oxygen levels modulate iron-regulatory protein activities in vivo. Science. 2004; 306:2087–2090. (see comment). [PubMed: 15604406]

Miller DS. Confocal imaging of xenobiotic transport across the choroid plexus. Adv Drug Delivery Rev. 2004; 56:1811–1824.

Moos T, Morgan EH. The significance of the mutated divalent metal transporter (DMT1) on iron transport into the Belgrade rat brain. J Neurochem. 2004; 88:233–245. [PubMed: 14675167]

Reaney SH, Smith DR. Manganese oxidation state mediates toxicity in PC12 cells. Toxicol Appl Pharmacol. 2005; 205:271–281. [PubMed: 15922012]

Roth JA, Horbinski C, Feng L, Dolan KG, Higgins D, Garrick MD. Differential localization of divalent metal transporter 1 with and without iron response element in rat PC12 and sympathetic neuronal cells. J Neurosci. 2000; 20:7595–7601. [PubMed: 11027219]

Rouault TA. Systemic iron metabolism: a review and implications for brain iron metabolism. Pediatr Neurol. 2001; 25:130–137. [PubMed: 11551743]

Rouault TA, Klausner RD. The impact of oxidative stress on eukaryotic iron metabolism. EXS. 1996; 77:183–197. [PubMed: 8856975]

Siddappa AJ, Rao RB, Wobken JD, Leibold EA, Connor JR, Georgieff MK. Developmental changes in the expression of iron regulatory proteins and iron transport proteins in the perinatal rat brain. J Neurosci Res. 2002; 68:761–775. [PubMed: 12111837]

Siddappa AJ, Rao RB, Wobken JD, Casperson K, Leibold EA, Connor JR, Georgieff MK. Iron deficiency alters iron regulatory protein and iron transport protein expression in the perinatal rat brain. Pediatr Res. 2003; 53:800–807. [PubMed: 12621119]

Su MA, Trenor CC, Fleming JC, Fleming MD, Andrews NC. The G185R mutation disrupts function of the iron transporter Nramp2. Blood. 1998; 92:2157–2163. [PubMed: 9731075]

Takeda A, Takatsuka K, Sotogaku N, Oku N. Influence of iron-saturation of plasma transferrin in iron distribution in the brain. Neurochem Int. 2002; 41:223–228. [PubMed: 12106773]

Vidal S, Belouchi AM, Cellier M, Beatty B, Gros P. Cloning and characterization of a second human NRAMP gene on chromosome 12q13. Mamm Genome. 1995; 6:224–230. [PubMed: 7613023]

Walker NJ. Real-time and quantitative PCR: applications to mechanism-based toxicology. J Biochem Mol Toxicol. 2001; 15:121–127. [PubMed: 11424221]

Zheng W, Zhao Q. Iron overload following manganese exposure in cultured neuronal, but not neuroglial cells. Brain Res. 2001; 897:175–179. [PubMed: 11282372]

Zheng W, Zhao Q. Establishment and characterization of an immortalized Z310 choroidal epithelial cell line from murine choroid plexus. Brain Res. 2002; 958:371–380. [PubMed: 12470873]

Zheng W, Ren S, Graziano JH. Manganese inhibits mitochondrial aconitase: a mechanism of manganese neurotoxicity. Brain Res. 1998; 799:334–342. [PubMed: 9675333]

Zheng W, Zhao Q, Slavkovich V, Aschner M, Graziano JH. Alteration of iron homeostasis following chronic exposure to manganese in rats. Brain Res. 1999; 833:125–132. [PubMed: 10375687]

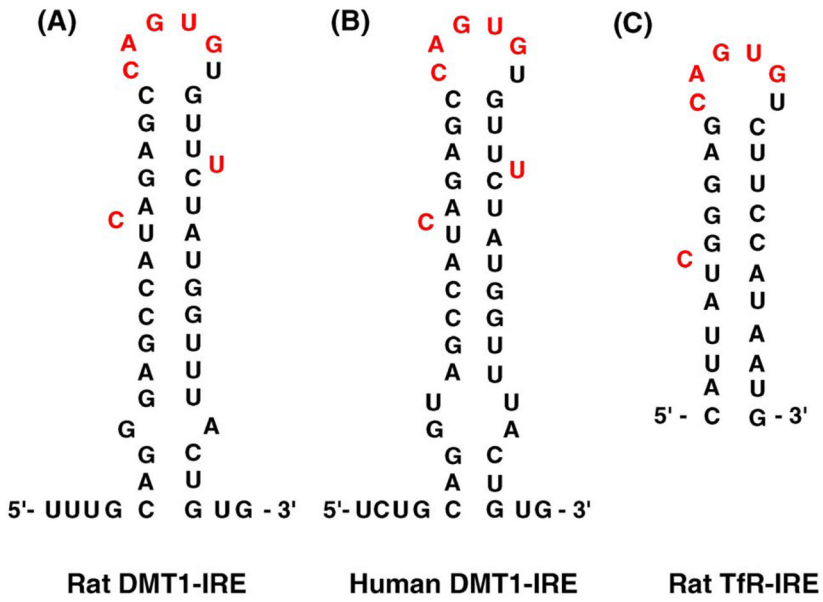

Fig. 1.

Stem-loop structures of iron responsive element (IRE) in mRNA encoding DMT1 and TfR. (A) Rat DMT1-IRE; (B) human DMT1-IRE; and (C) rat TfR-IRE.

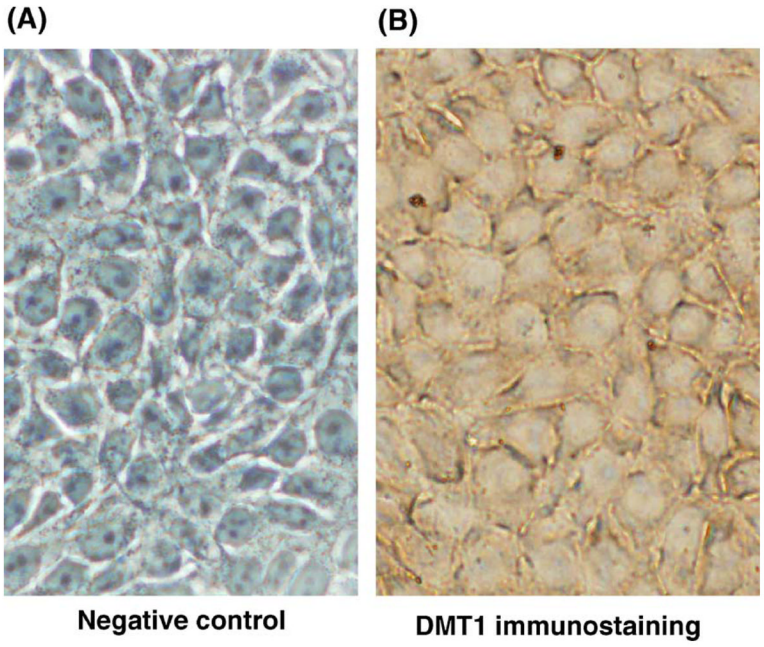

Fig. 2.

Immunocytochemical staining of DMT1 in cultured Z310 cells. The cells were cultured on Lab-Tek II chamber slide and incubated without (A) or with (B) antibody against DMT1 followed by reaction with biotinylated antibody. The punctate staining of DMT1 was seen in the cytoplasm of Z310 cells (B) (×200).

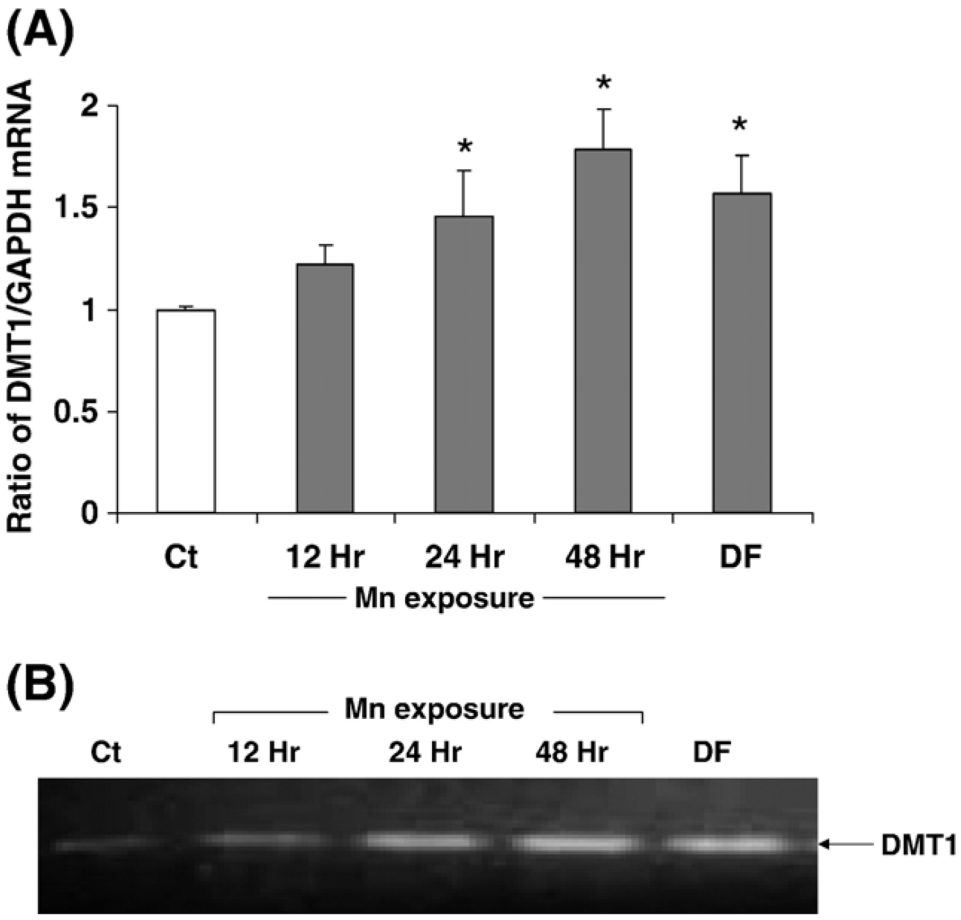

Fig. 3.

Expression of DMT1 mRNA in Z310 cells as affected by manganese exposure. Z310 cells were treated with 100 μM $MnCl_2$ for 12, 24 or 48 h or with 50 μM DFOM for 10 h as a positive control. (A) DMT1 and GAPDH mRNA levels were quantified by real-time RT-PCR and expressed as the ratio of DMT1/GAPDH. Data represent mean ± SE, $n = 3$; *$P <$ 0.05 as compared to control. (B) Representative bands were shown on an agarose gel.

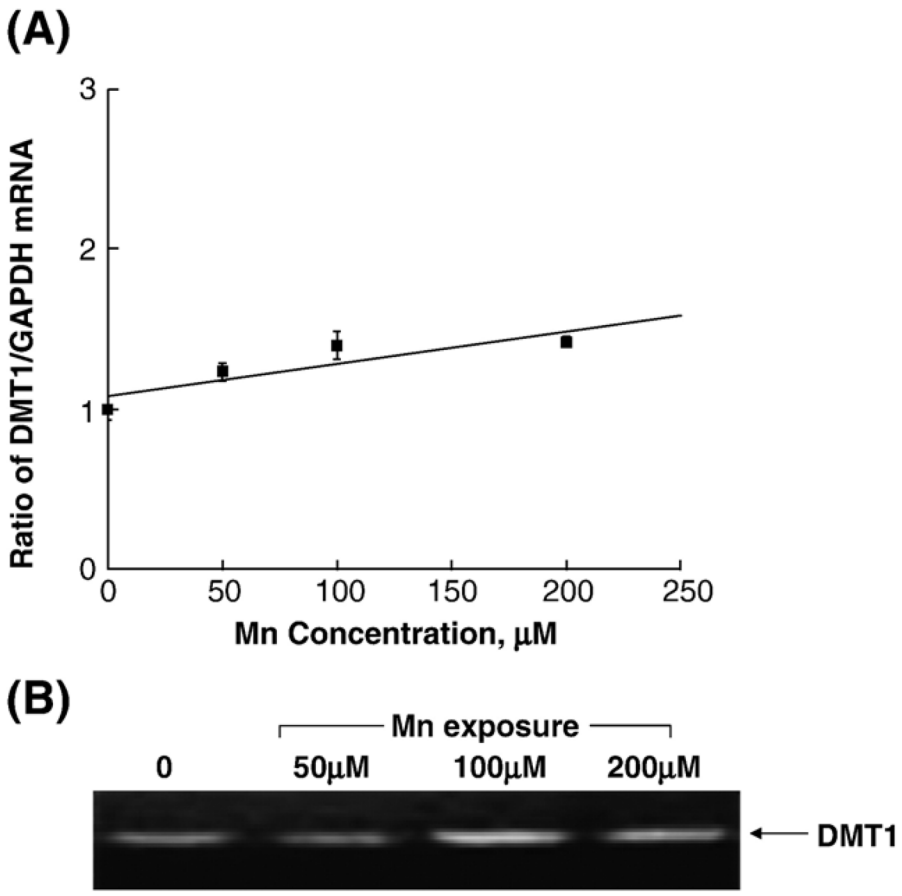

Fig. 4.

Dose–response relationship of manganese effect on the expression of DMT1 mRNA in Z310 cells. Z310 cells were treated with 50, 100 or 200 μM $MnCl_2$ for 24 h. (A) DMT1 and GAPDH mRNA levels were quantified by real-time RT-PCR and expressed as the ratio of DMT1/GAPDH. Data represent mean ± SE, $n = 3$, correlation coefficient (r) = 0.870, $P < 0.01$. (B) Representative bands were shown on an agarose gel.

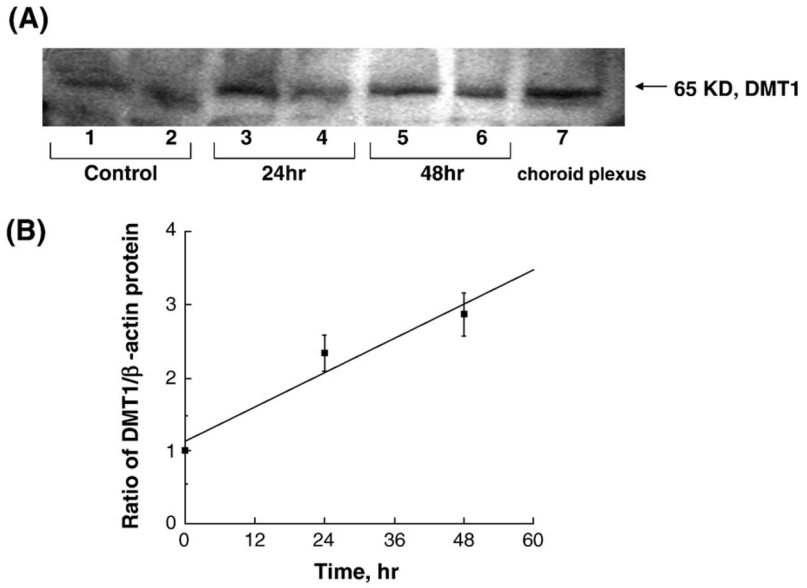

Fig. 5.

Expression of DMT1 protein in Z310 cells by Western blot analyses. (A) Z310 cells were treated with 100 μM $MnCl_2$ for 0 h (Ct as control), 24 h and 48 h. Lanes 1, 3, 5: Z310 passage 59 were used; lanes 2, 4, 6: Z310 passage 221 were used; lane 7: choroid plexus tissue. The autograph is a representative of triplicate experiments. (B) Time course of manganese effect on DMT1 protein expression. DMT1 protein levels were normalized to β-actin. Data represent mean ± SE, $n = 3$; $P < 0.05$ as compared to control; correlation coefficient (r) = 0.971, $P < 0.01$.

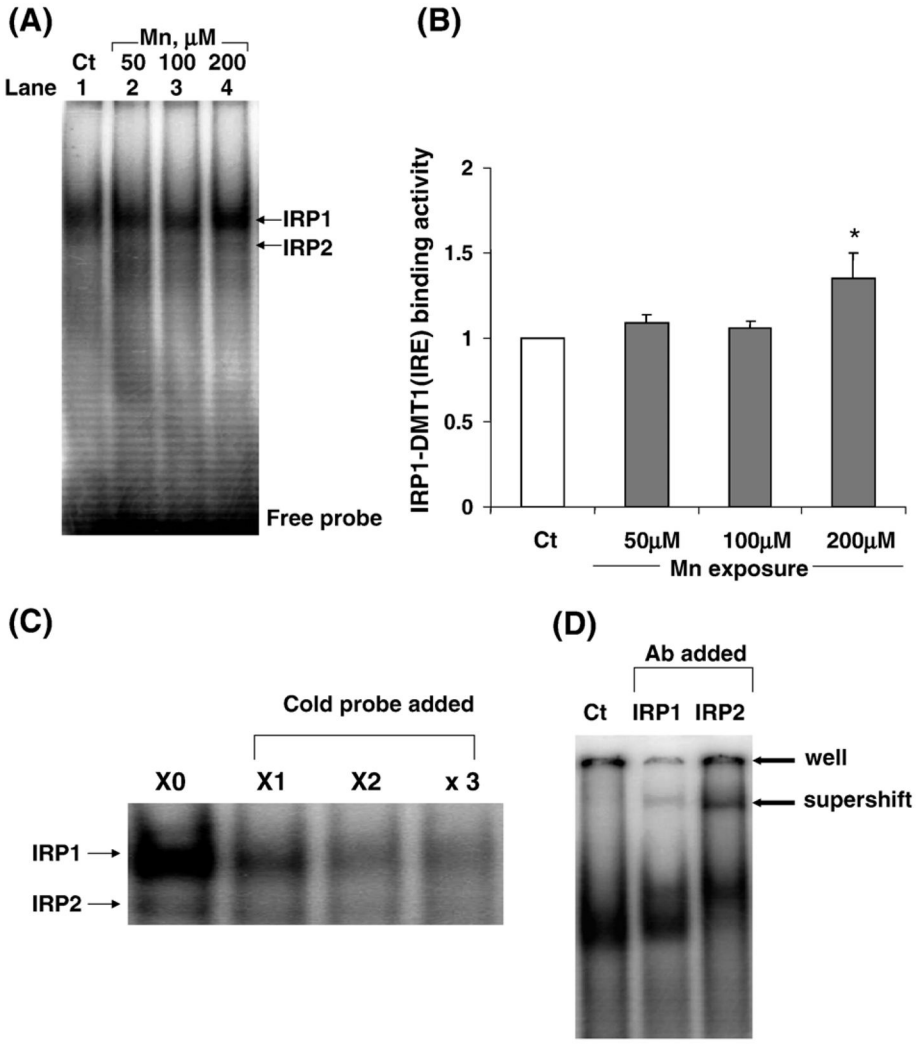

Fig. 6.

Binding of IRPs to DMT1-IRE as affected by manganese exposure. Z310 cells were treated with 50, 100 or 200 μM $MnCl_2$ for 24 h. EMSA was performed by incubating ^{32}P-labeled DMT1-IRE with 10 μg cytoplasmic preparation. (A) A representative autoradiograph of binding of IRP1 to DMT1 mRNA. Arrow indicates a shifted protein–mRNA complex band. (B) The densities of bands were quantified and expressed as IRP1-DMT1 (IRE) binding activity. Data represent mean ± SE, $n = 3$; *$P < 0.05$ as compared to controls. (C) Competition study with unlabeled DMT1-IRE. The EMSA was conducted in the presence of 1×-, 2×-, 3×-fold excess of unlabeled competitor DMT1-IRE. (D) Supershift assay by incubating the cytoplasmic preparation with antibody against IRP1 or IRP2 prior to EMSA. Data in (C) and (D) suggest a specific interaction between IRP1 and IRE-containing DMT1 mRNA.

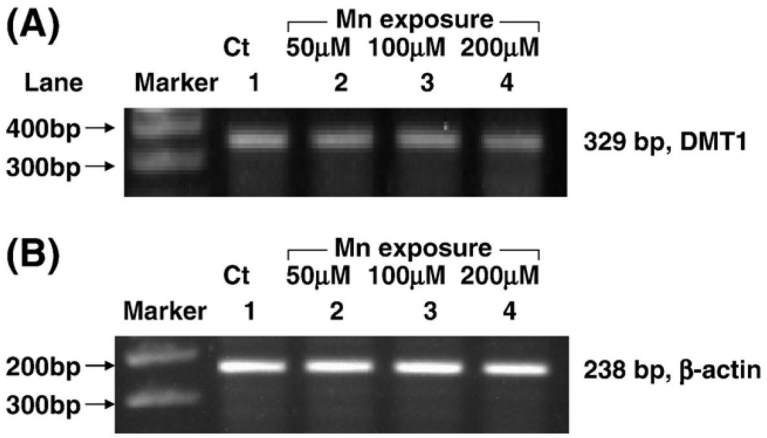

Fig. 7.

Lack of effect of manganese exposure on DMT1 hnRNA by real-time RT-PCR analyses. (A) DMT1 hnRNA; (B) β-actin hnRNA. Z310 cells were treated with 0 μM (lane 1), 50 μM (lane 2), 100 μM (lane 3), 200 μM (lane 4) of $MnCl_2$ for 24 h.